PNAS
www.pnas.org

Supplementary Information for

EXO70D isoforms mediate selective autophagic degradation of Type-A ARR proteins to regulate cytokinin sensitivity

Atiako Kwame Acheampong[1a], Carly Shanks[1a], Chai-Yi Chang[1], G. Eric Schaller[2], Yasin Dagdas[3], and Joseph J. Kieber[1]*

Corresponding author: Joseph J. Kieber
Email: jkieber@unc.edu

This PDF file includes:

Figures S1 to S7
Tables S1

www.pnas.org/cgi/doi/10.1073/pnas.2013161117

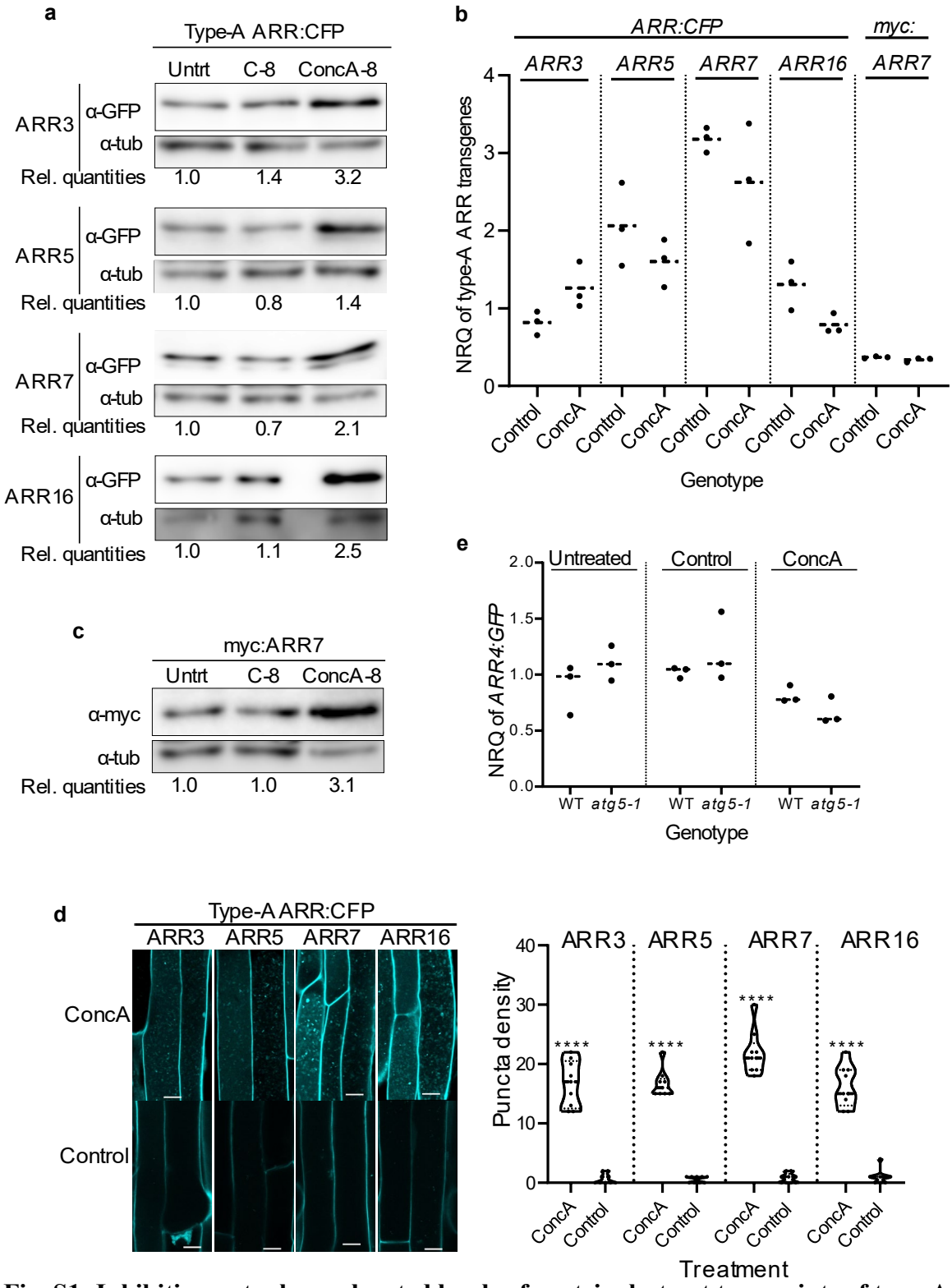

Fig. S1: Inhibiting autophagy elevated levels of protein, but not transcripts of type-A ARR. (*A*) Immunoblot assays of ectopically-expressed type-A ARRs in response to

ConcA. Ten-day old *Arabidopsis* seedlings carrying *pUBQ10::ARR:CFP* constructs were treated for 8 h in sucrose-deficient liquid MS media supplemented with 1 μM ConcA (ConcA-8) or vehicle control (C-8). ARR protein quantities in treated roots, relative to untreated roots (Untrt), were analyzed by immunoblot assays using anti-GFP (α-GFP) antibodies. Anti-tubulin (α-tub) served as loading control. Rel. quantities represent ratio of intensity of α-GFP to α-tub band relative to ratio of Untrt bands for each blot. **(*B*)** qRT-PCR analyses of transcript levels of *pUBQ10::ARR:CFP* transgene in roots of seedlings described in **Fig. S1*A*** above. **(*C*)** Immunoblot analyses of ectopically-expressed myc:ARR7 protein in roots of seedling in the presence of ConcA. myc:ARR7 levels were assayed using α-myc antibodies. **(*D*)** Representative confocal micrograph of the root elongation zones of *Arabidopsis* seedlings carrying CFP-tagged type-A ARR constructs. The light grown seedlings treated with ConcA (***Upper panels***) or DMSO as vehicle control (***Lower panel***) and exposed to carbon starvation for 18 h prior to imaging. Scale bar =10 μm. Quantification of the number of CFP-containing vacuolar vesicles. Data represents the average number of puncta per 100 μm^2 of vacuole area, n=8. Statistical differences between treatments were analyzed using students'*t*-test. **** represent statistically different means at $p<0.05$. **(E)** qRT-PCR analyses of transcript of *pUBQ10::ARR4:GFP* transgene in roots of seedlings of wild-type and autophagy-deficient mutant, *atg5-1*, treated with ConcA for 1 h. For **Fig. S1*B*** and **Fig. S1*E***, plots represent the mean normalized relative quantities (NRQ) of three biological replicates. Filled black circles and broken lines represent individual value and mean values, respectively. Statistical differences between genotypes was analyzed by Students' *t*-test; $p<0.05$.

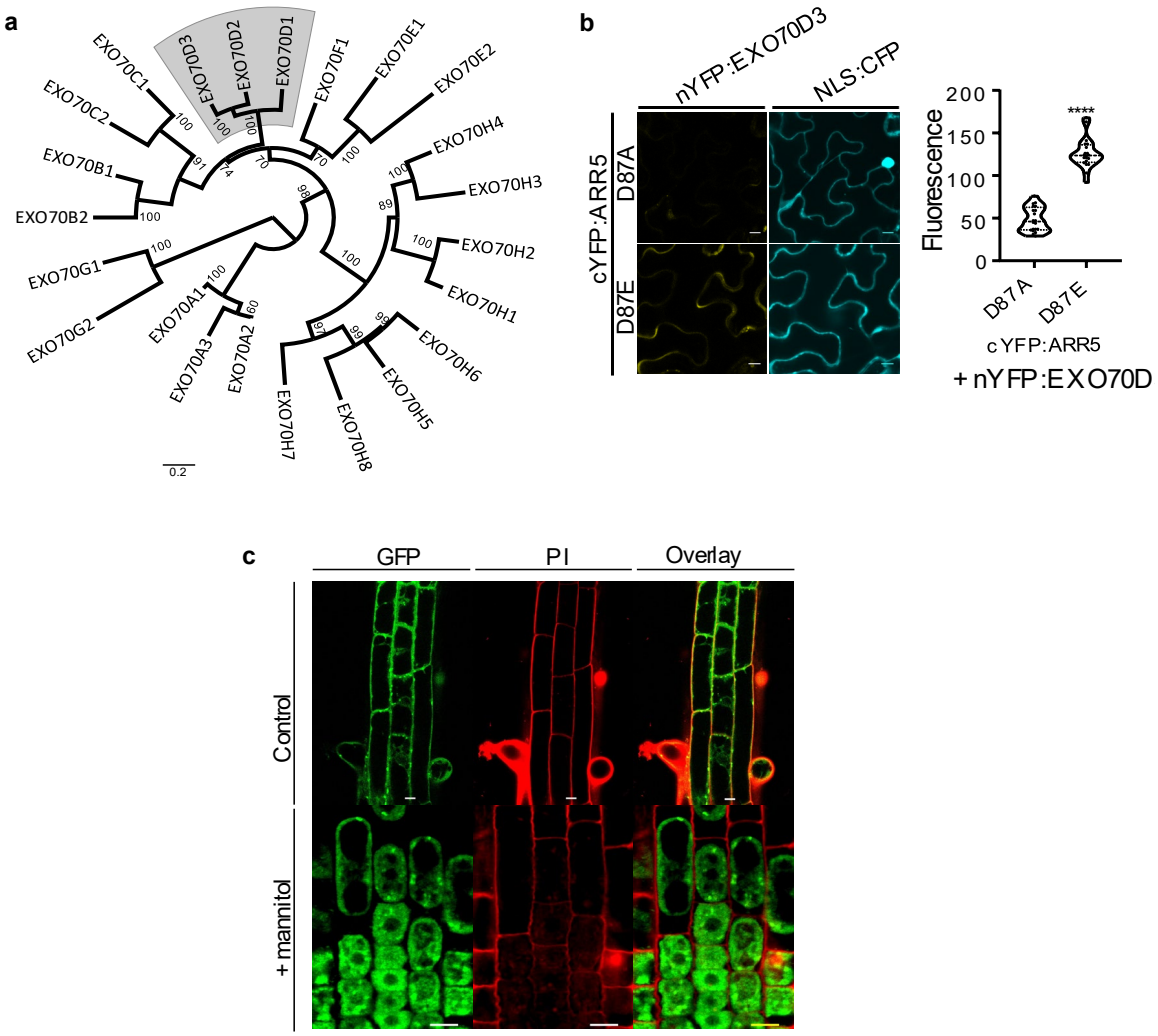

Fig. S2: EXO70D3, a member of the EXO70 gene family, interacts with type-A ARRs in a phospho-Asp dependent manner. (*A*) Phylogenetic tree showing the amino acid relatedness of 23 members of the EXO70 gene family. The genes cluster into three main clades, and nine subclades consisting of 3 EXO70As, 2 EXO70Bs, 2 EXO70Cs, 3 EXO70Ds, 2 EXO70Es and a single EXO70F1, 2 EXO70Gs, EXO700H1-EXO70H4, and EXO70H5-EXO70H8. The three isoforms of the EXO70D sub-clade are highlighted by grey halo. The radial tree was created by the web-based Phylogeny (1) using Neighbor-joining algorithm. To generate the tree, the amino acid sequences were aligned using

MUSCLE (2), and curated using Gblocks (3) and the phylogeny created using PhyML (4). Tree Rendering was performed using TreeDyn (5). Bootstrap values represent 1000 iterations. Scale bar represents 0.2 amino acid substitutions per site. **(*B*)** Confocal micrograph of bimolecular fluorescence complementation (BiFC) assay depicting the interaction of EXO70D3 with the phospho-dead (D87A) and phospho-mimic (D87E) mutants of ARR5 in epidermal cells of *Nicotiana benthamiana* leaves. D87A and D87E mutations represent site-directed mutagenesis of the conserved Aspartate on the ARR5 to Alanine and Glutamate, respectively. EXO70D3 and ARR5 were tagged with N-terminus (nYFP) and C-terminus of split YFP (cYFP), respectively. NLS:CFP, a CFP-tagged nuclear localizing sequence was used as a infiltration control. Scale bar = 10μM. Quantification of the fluorescent intensities from images was performed with Fiji software. Data indicate the average of the maximum intensity values of the YFP signal relative to the corresponding CFP signals of 20 images for each infiltration. **** indicates statistically significant differences at $p<0.001$. **(*C*)** Confocal images showing EXO70D3:GFP protein predominantly localize in the cytoplasm of roots of four-day old *Arabidopsis* seedling. Seedlings carrying *pUBQ10::EXO70D3:GFP* construct were plasmolyzed by incubating for 90 min in MS media supplemented with 0.8 M mannitol and subsequently stained with propidium iodide for 1 min prior to imaging. Left panel indicates GFP channel, while middle and right panels represent propidium iodide (PI) and merged images, respectively. Plasmolyzed seedlings are shown in lower panel.

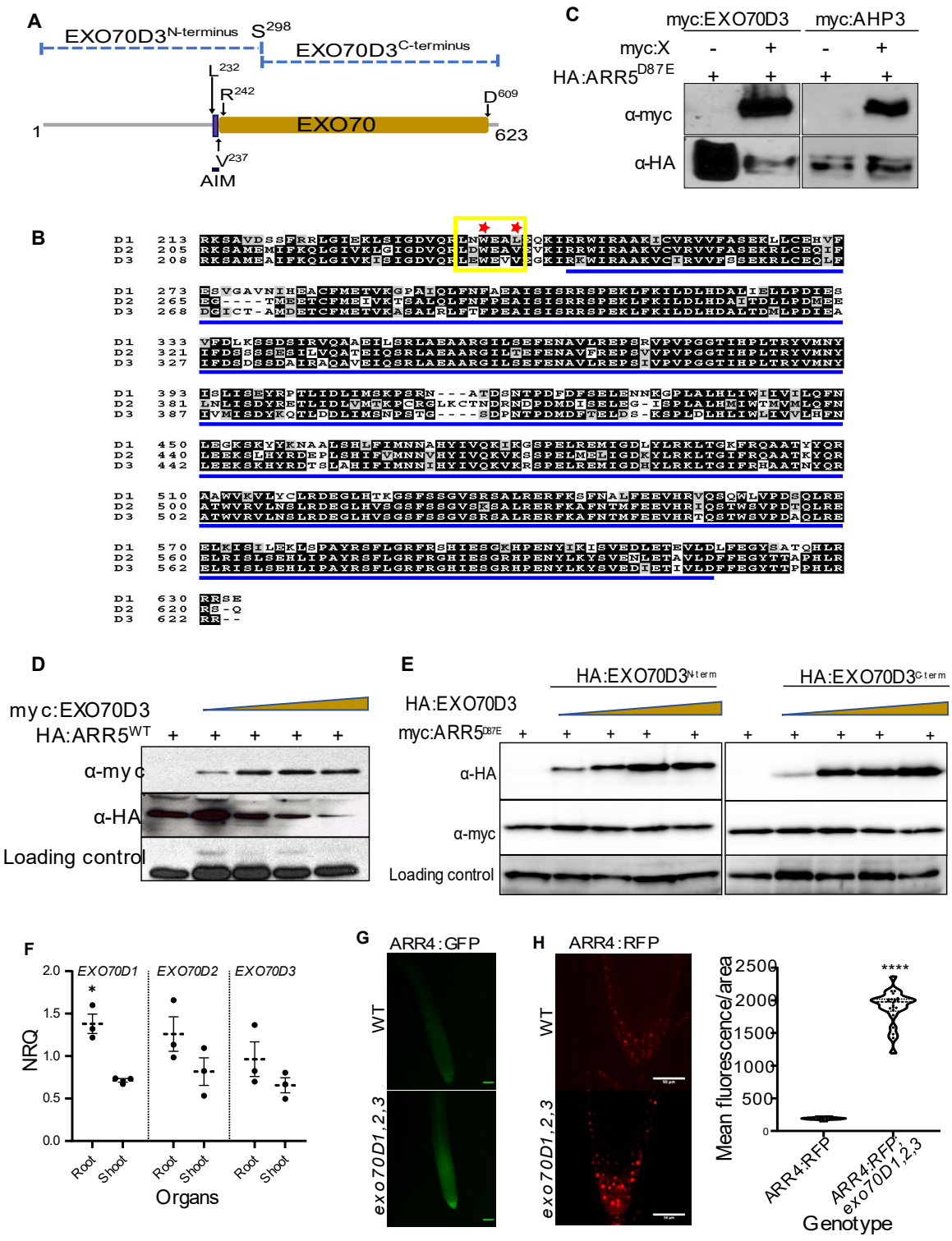

Fig. S3: Full-length EXO70D3 destabilizes type-A ARRs *in planta*. (*A*) A modified schematic representation of EXO70D3 as generated by the iLIR database[4] and indicating ATG8-interacting motif (AIM) (232-LEWEVV-237) and an EXO70 domain (R^{242}-D^{609}).

Three low complexity regions (S^{59}-A^{77}; A^{148}-R^{171}; S^{518}-S^{529}) were also identified (not indicated in Figure). In this study, interaction and co-expression assays were carried out using the AIM-containing EXO70D3$^{N\text{-terminus}}$ fragment, and the rest of the protein, EXO70D3$^{C\text{-terminus}}$. **(*B*)** Alignment of amino acid sequences of EXO70D isoforms. Yellow box and blue lines indicate predicted AIMs and EXO70 domain, respectively. Red stars denote the conserved residues in the predicted AIM. Black background indicates consensus residues. **(*C*)** Co-expressing phospho-mimic ARR5 (ARR5^{D87E}) with full length EXO70D3 in leaves of *N. benthamiana* results in decrease in ARR5^{D87E} protein levels. HA:ARR5^{D87E} was co-infiltrated with equivalent amounts myc:EXO70D3 (***left panel***) or myc:AHP3 (***right panel***). **(*D*)** Full length EXO70D3 destabilizes ARR5 proteins in a concentration dependent manner. *N. benthamiana* leaves were transiently co-transformed with fixed amount of HA:ARR5 and increasing titer of myc:EXO70D3. **(*E*)** Co-expressing partial-length EXO70D3 does not result in the decrease in ARR5 proteins, regardless of the phosphorylation status of the conserved Aspartate. Phospho-mimic ARR5 (ARR5^{D87E}) is co-expressed with N-terminal (EXO70D3$^{N\text{-term}}$) (***Left panel***) and C-terminal (EXO70D3$^{C\text{-term}}$) (***Right panel***) truncations of EXO70D3. **(*F*)** qRT-PCR analyses of transcript levels of *EXO70D1*, *EXO70D2* and *EXO70D3* in *Arabidopsis* wild-type seedling roots and shoots. Plots represent the mean normalized relative quantities (NRQ) of three biological replicates with SEM. Statistical differences between values of root and shoot was analyzed by Student' *t*-test, $P < 0.05$. Asterisk (*) indicate significant differences between root and shoot expression at $p = 0.0139$. **(*G*)-(*H*)** Disrupting *EXO70Ds* resulted in accumulation of type-A ARR proteins in *Arabidopsis*. Plants expressing *pUBQ10::ARR4:GFP* or *pUBQ10::ARR4:RFP* were crossed to *exo70D1,2,3* triple loss-of-function mutants to

produce ARR4:GFP;*exo70D1,2,3* or ARR4:RFP;*exo70D1,2,3* plants**.** Confocal microscopy images indicating the expression of pUBQ10::ARR4:FP in whole root **(*G*)** and root tip **(*H*)** of wild-type (***top panel***) and *exo70D1,2,3* mutant (***bottom panel***) plants. Scale bars = 100 μm and 50 μm for **(*G*)** and **(*H*)**, respectively. For **(*H*),** the signal intensity of individual nuclei were quantified. The graph represents the average signal measurement from 22 images of each genotype. Data was analyzed by unpaired Student's t-test. **** indicate statistical difference at p=2.979x10^{-030}

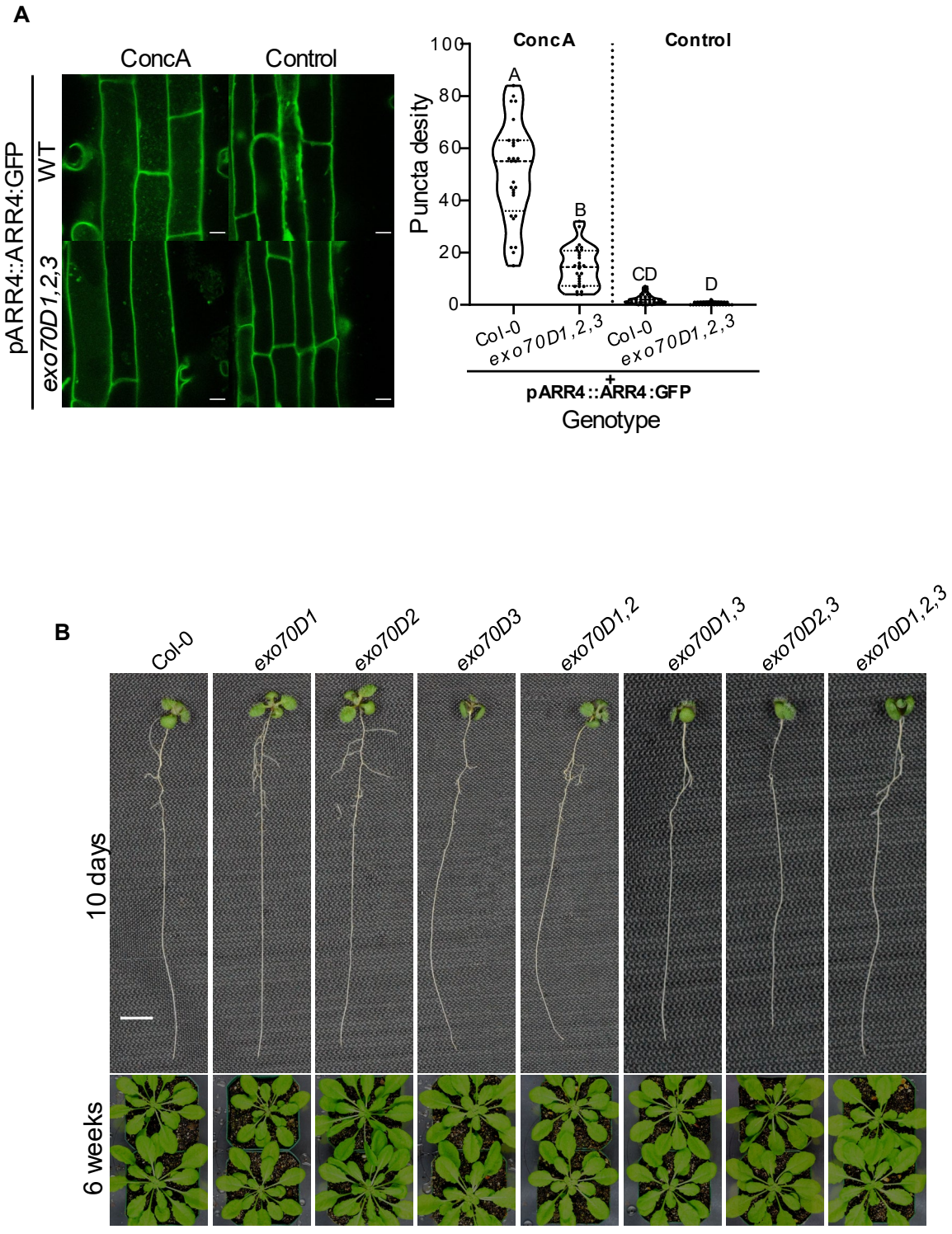

Fig. S4: EXO70D genes traffic type-A RRs into the vacuole, but do not significantly alter plant morphology: (*A*) Representative confocal micrograph of the root elongation zones of T1 seedlings of wild-type Col-0 (***upper panel***) and *exo70D1,2,3* mutant (***lower***

panel) transformed with ARR4 fusion protein driven by ARR4 native promoter (pARR4::ARR4:GFP). Seedlings were grown in light for 5 days on MS plates supplemented with 50 µg/mL hygromycin, followed by incubation with 1 µM ConcA (***left panel***) or DMSO (***right panel***) under carbon starvation conditions for 18 h. Scale bar =10 µm. For each genotype and treatment, 28 independent T1 seedlings were used. Three images were collected from each seedling. Using ImageJ software, the number of GFP-containing puncta was computed from the uppermost 5000 μm^2 area of each image. Data (n=84) was analyzed with one-way ANOVA followed by Tukey-Kramer multiple comparison analyses; $p<0.05$. Different letters represent values that are statistically different at the indicated *p*-value. **(*B*)** Comparative morphologies of 10-day and 6-week old wild type (Col-0) and *exo70D* mutants. Ten-day-old seedlings were grown under continuous light on vertical plates, while 6-week-old plants were grown under short day conditions in pots. Scale bar = 0.5 cm (for 10-day old seedlings); and 2 cm (for 6 weeks old).

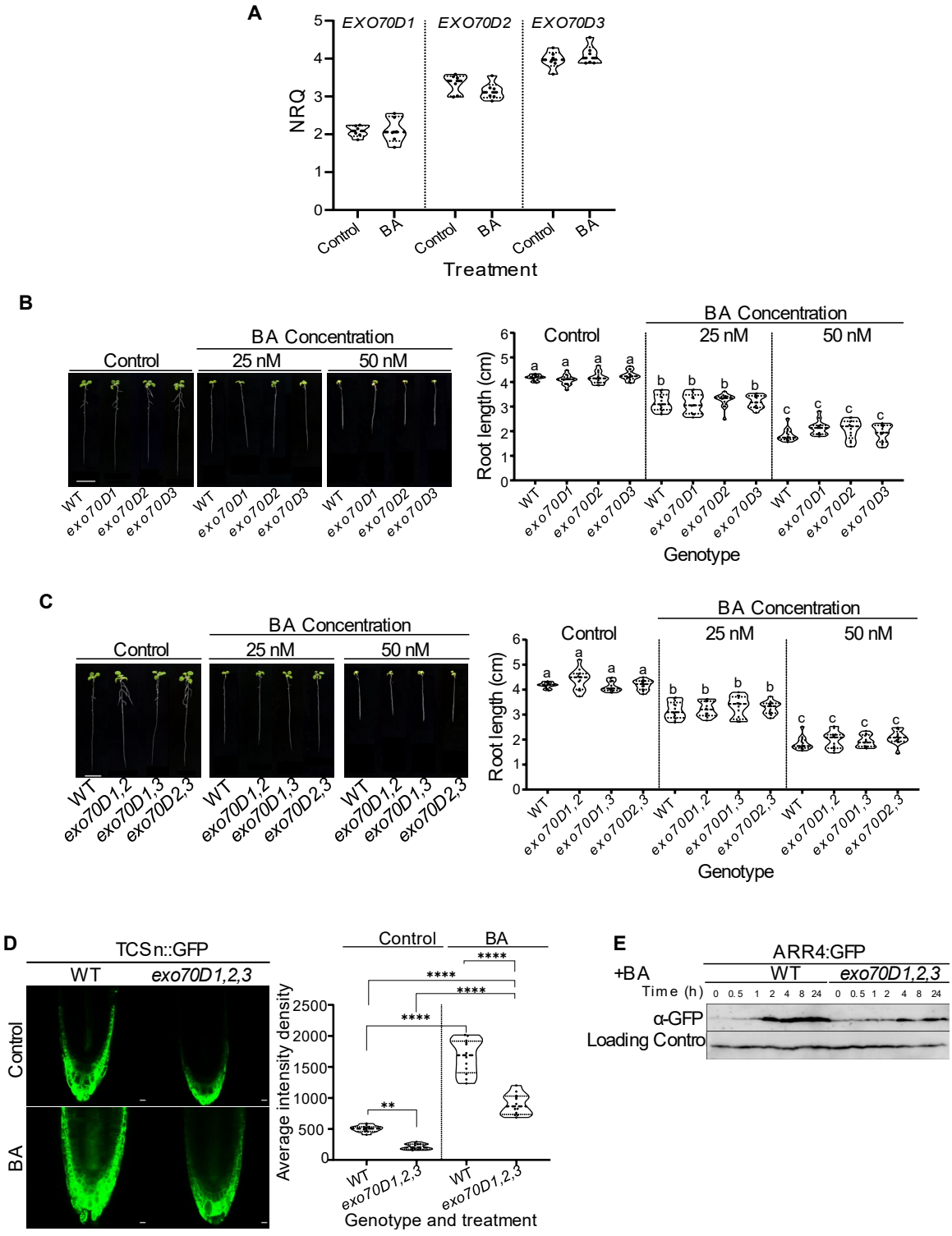

Fig. S5: Interplay between cytokinin and EXO70Ds in *Arabidopsis* root. (*A*) Cytokinin does not alter transcript levels of *EXO70D* isoforms. qRT-PCR analyses of transcript levels of *EXO70D1*, *EXO70D2* and *EXO70D3* in *Arabidopsis* roots treated with BA or NaOH

(Control)**.** Plot represents NRQ values of expressions in BA-treated and Control samples from three biological replicates with two technical replicates each. Statistical differences between treatments was analyzed by unpaired Students' *t*-test. **(*B-D*)** Effect of cytokinin on the length of primary roots of single (*exo70D1*, *exo70D2*, *exo70D3*) **(*B*)** and double (*exo70D1,2*, *exo70D1,3*, *exo70D2,3*) **(*C*)** loss-of-function mutants of *EXO70D* genes. Seedlings were grown on vertically on MS plates, and after 4 days transferred to plates supplemented with 6-benzyl-adenine (BA) or NaOH plates as a vehicle control for 6 days. Violin plots show quantitation of the primary root length in response to different BA concentrations. Values represent the average of more than 11 measurements, analyzed with one-way ANOVA followed by Tukey-Kramer multiple mean comparisons at $p<0.05$. **(*D*)** Disrupting all three *EXO70D* genes reduces the type-B ARR activity in *Arabidopsis* roots. Confocal microscopy images showing expression of the type-B RR reporter TCSn::GFP in wild type (***left panels***) and *exo70D1,2,3* triple mutant (***right panels***) plants incubated in 5µM BA (***lower panels***) or NaOH control media (***upper panels***) for 2h. Scale bar = 50 µm. Intensity of the GFP signal from more than 11 determinations (n≥11) was analyzed with two-way ANOVA and Sidak's comparisons; $P < 0.05$. ** and **** indicate significant differences at $P=0.0022$ and $P<0.0001$, respectively. **(*E*)** Effect of BA treatment on ARR4:GFP protein levels in wild-type and *exo70D1,2,3* mutant seedlings. Proteins extracted from 10-day old seedlings following treatment with cytokinin (BA) for up to 24 h, were analyzed by immunoblot assay using anti-GFP. Anti-tubulin (α-tub) served as loading control.

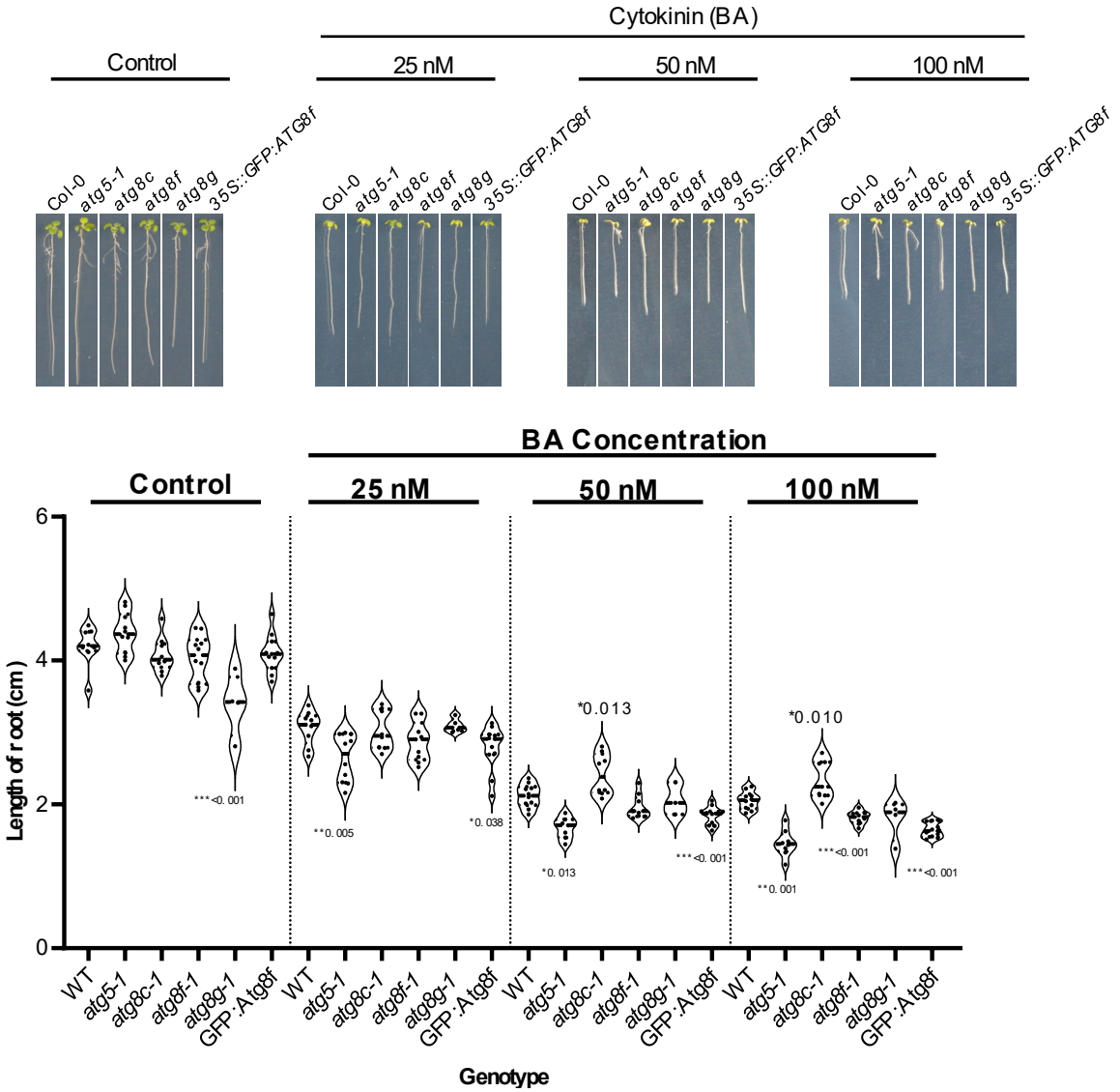

Fig. S6: Effect of altered *ATG* expression on response to exogenous cytokinin: Root elongation assay showing effect of mis-regulation of *ATG* genes on perception of cytokinin. Seedlings were grown on MS media for 4 days, and transferred to MS media supplemented with BA (cytokinin) or NaOH (control) for 5 days. Scale bar = 1 cm. Plants were imaged, and root length measured using FIJI software. Graph represents average length (n≥8) at each concentration. * indicates means of root lengths that are statistically different from wild-type roots at $p<0.05$. The assay was conducted twice with similar results.

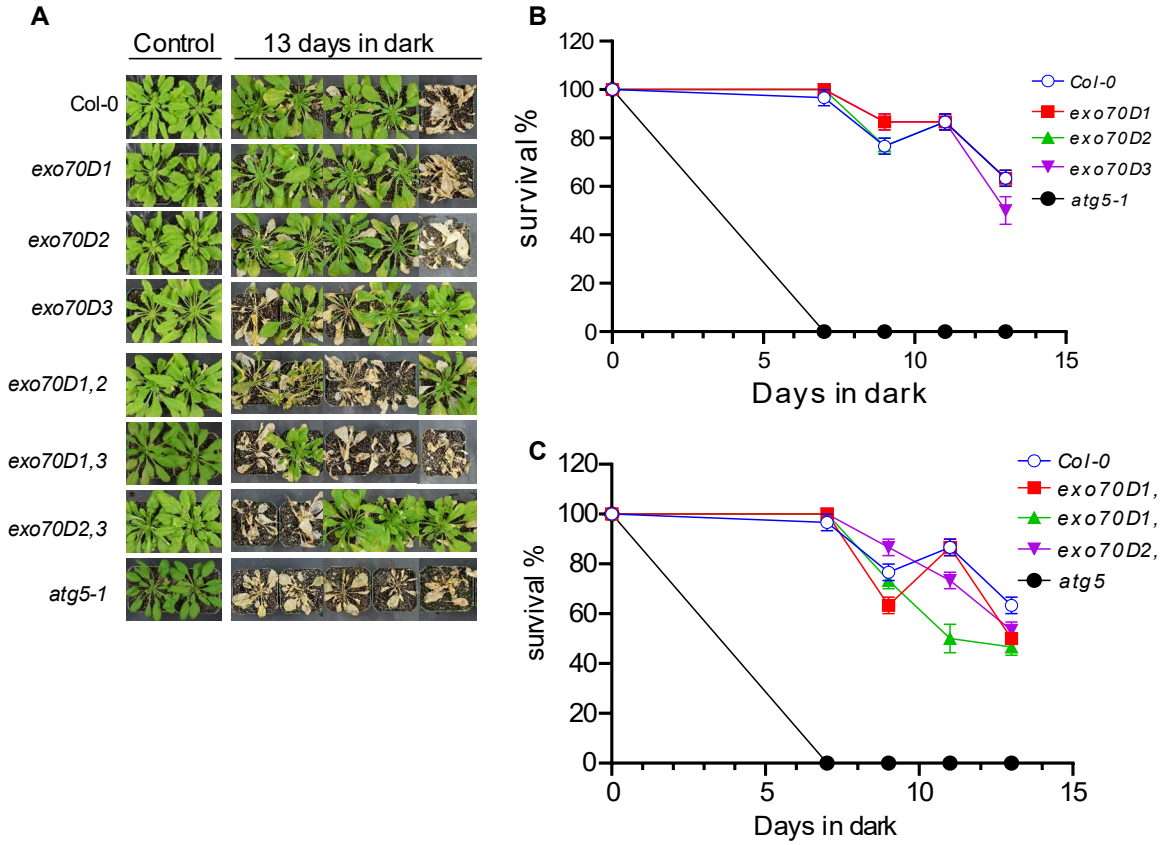

Fig. S7: Responses of lower order mutants of *EXO70D*s to fixed-carbon starvation. Seedlings were grown for six weeks on potted soil under short-day conditions, and transferred to dark for 7, 9, 11, 13 days. Plants were recovered in the light (short day) for 7 days. **(*A*)** Representative images of single (*exo70D1, exo70D2, exo70D3*) and double (*exo70D1,2*; *exo70D1,3*; *exo70D2,3*) loss-of-function mutants of *EXO70D*s following 13-day-dark treatment. Col-0 and *atg5-1* served as wild-type and autophagy deficient controls, respectively. Graphical representation of quantification of survival of single **(*B*)** and double **(*C*)** mutants in response to carbon starvation. Survival was estimated as the percentage of plants with new leaves after the dark treatment. Values represent mean ± SEM percentage survival of 3 biological replicates. Each biological replicate consisted of 8 plants per genotype per treatment.

Table S1: Primers used in this study

Gene	Forward primer (5'→3')	Reverse primer (5'→3')	Purpose
exo70D1	ggatcgtcttctcagatgctg	tgctctgtgagcatgtttttg	T-DNA genotyping
exo70D2	cgcattctcaaactcggtaag	attctgattatggcaacaccg	T-DNA genotyping
exo70D3	cgtctttaaccgtcgaagttg	ctgacccatgtagctctctgg	T-DNA genotyping
atg8c-1	gttaatgcgttttggtgcatc	gaaagagtgtgccttgctttg	T-DNA genotyping
atg8f-1	acttcaatggtccaaaatccc	ttttcattcggacctgacttg	T-DNA genotyping
atg8g-1	ccgatttgatttcgtttatgc	ttggttgtgcctacataagcc	T-DNA genotyping
atg5-1	atttgctatttgtttggcacg	taccgttcatgacagaggtcc	T-DNA genotyping
arr3	ggaactagtagcaatatctctcttctatcttttc	cacagaggtaaactgtcacacattatttg	T-DNA genotyping
arr4	tttatgtgcgacacgttgatgactacttt	ggaggcgcgagagattaaagggacatctat	T-DNA genotyping
arr5	tctctctgtggtacatttcttgaaaaatggg	cttggggaaatttctaagaaaagccatgta	T-DNA genotyping
arr6	tgtagaagttaaatgcgtgaacttccaca	gctatggtgaatcctcttgacaagttactc	T-DNA genotyping
arr7	ggcggtttgcagactcacttacctga	gactctctcaaacattgtcttt	T-DNA genotyping
arr8	caaatggctgttaaaacccaccaata	ccattgttagtgtgctatcacctgagtg	T-DNA genotyping
arr9	ggatcccagactctttatttctcttcctc	cccacatacaacatcatcatcatattcc	T-DNA genotyping
arr15	ccatttattctcctctcatctc	atctaatcatccccatctcc	T-DNA genotyping
EXO70D1	caccatggaaccacatgaccaaactcacg	tcactcggatcgtcttctcagatgc	Cloning full-length CDS
EXO70D2	caccatggcaacaccggagact	tcactgagaccgtctcaaa	Cloning full-length CDS
EXO70D3	caccatggaaccgccggagaat	ttatcgcctcctcaagtgtggt	Cloning full-length CDS
ATG8a	caccatgatctttgcttgcttga	tcaagcaacggtaagagatc	Cloning full-length CDS
ATG8b	caccatggagaagaactccttca	ttagcagtagaaagatccac	Cloning full-length CDS
ATG8c	caccatggctaatagctctttca	ctaagaagttgtgtgtttac	Cloning full-length CDS
ATG8d	caccatggcgattagctccttca	ttagaagaagatcccgaacg	Cloning full-length CDS
ATG8e	caccatgaataaaggaagcatct	ttagattgaagaagcaccga	Cloning full-length CDS
ATG8f	caccatggcaaaaagctcgttcaa	ttatggagatccaaatccaa	Cloning full-length CDS
ATG8g	caccatgagtaacgtcagcttcag	ttaagtcattgacgatccaa	Cloning full-length CDS
ATG8h	caccatggggattgttgtcaagt	ttagccgaaagttttctcgg	Cloning full-length CDS
ATG8i	caccatgaaatcgttcaaggaac	tcaaccaaaggttttctcac	Cloning full-length CDS
mCherry:ATG8e	aacaggtctcaggctctatgaata aaggaagcatctttaagatg	aacaggtctcactgagattgaa gaagcaccgaatgt	Cloning full-length CDS for Greengate cloning
EXO70D3$^{N\text{-}term}$	caccatggaaccgccggagaat	ttaacttatagcttcaggg	Cloning CDS
EXO70D3$^{C\text{-}term}$	caccatgatcagtagaagatcacctg	ttatcgcctcctcaagtgtggt	Cloning CDS
mut- EXO70D3	gcttgagGCggaagttgC tgaaggaaagatcagg	ccttcaGcaacttccGC ctcaagcctttgaacat	Generating SDM in AIM
AHP2	caccatggacgctctcattgctca	ttagttaatatccacttgagg	Cloning full-length CDS
AHP3	caccatggacacactcattgctca	ttatatatccacttgagg	Cloning full-length CDS
ARR4	caccatggccagagacggtggt	ctaatctaatccgggactcc	Cloning full-length CDS
ARR5	caccatggctgaggttttgcgtc	ttagatctttgcgcgttttag	Cloning full-length CDS
ARR7	caccatggcggttggtgaggt	tcaaagtagagaaaaaaggtt	Cloning full-length CDS
ARR16	caccatgaacagttcaggaggttc	ttagcttctgcagttcatga	Cloning full-length CDS
gARR4	cacccgattttatgtgcgacacgttg	atctaatccgggactcctcatcttc	Cloning ARR4 genomic fragment
mCherry_Spe1_F	tccaactagtatggtgagcaagggcgagg		Cloning full-length CDS with *Spe1* and *Mun1* sites

mCherry_Mun1_R		gattaacaattgcttgtacagctcgtcca	Cloning full-length CDS with *Spe1* and *Mun1* sites
EXO70D1	aatggtctccgccggttatc	agcgcttcccaatttagcct	qRT-PCR
EXO70D2	agactcgtggcgttgattcc	cttctcgatcaccaccgctt	qRT-PCR
EXO70D3	ggaaccgccggagaatagtt	atccacctcatcacgatcgc	qRT-PCR
ARR3:FP	tggttgacgatgaagattcg	accactttgtacaagaaagctgggt	qRT-PCR of transgene
ARR4:FP	gaagatgatgacgtgttgacg	accactttgtacaagaaagctgggt	qRT-PCR of transgene
ARR5:FP	ttaatgaaagctgaggaaagagc	accactttgtacaagaaagctgggt	qRT-PCR of transgene
ARR6:FP	tcacaaagagtattcagaagagagagc	accactttgtacaagaaagctgggt	qRT-PCR of transgene
ARR7:FP	gagaaagcttcaagaagacagtga	accactttgtacaagaaagctgggt	qRT-PCR of transgene
ARR9:FP	aacgttttcattgtgtcttgattc	accactttgtacaagaaagctgggt	qRT-PCR of transgene
ARR16:FP	agcgagtggagctcaaatgt	accactttgtacaagaaagctgggt	qRT-PCR of transgene
GAPDH	aggccatcaaggaggaatct	gaaaatgcttgacctgttgtcac	qRT-PCR

References

1. Dereeper A, Audic S, Claverie JM, & Blanc G (2010) BLAST-EXPLORER helps you building datasets for phylogenetic analysis. *BMC Evol. Biol.* 10:8.
2. Edgar RC (2004) MUSCLE: a multiple sequence alignment method with reduced time and space complexity. *BMC Bioinformatics* 5:113.
3. Guindon S & Gascuel O (2003) A simple, fast, and accurate algorithm to estimate large phylogenies by maximum likelihood. *Syst. Biol.* 52(5):696-704.
4. Castresana J (2000) Selection of conserved blocks from multiple alignments for their use in phylogenetic analysis. *Mol. Biol. Evol.* 17(4):540-552.
5. Chevenet F, Brun C, Bañuls AL, Jacq B, & Christen R (2006) TreeDyn: towards dynamic graphics and annotations for analyses of trees. *BMC Bioinformatics* 7:439.